

## Supporting Information

### Dynamic Inhomogeneity in Homogeneous Polymer Melts

Linlin Chu,<sup>a</sup> Kaipin Xu,<sup>a,c</sup> Robert Graf,<sup>b</sup> Zhi-Chao Yan<sup>\*d</sup>, Junfang Li<sup>\*e</sup> and Ye-Feng Yao<sup>\*a</sup>

<sup>a</sup> Physics Department & Shanghai Key Laboratory of Magnetic Resonance, School of Physics and Electronic Science, East China Normal University, North Zhongshan Road 3663, 200062 Shanghai, P.R. China.

<sup>b</sup> Max-Planck-Institute for Polymer Research, Ackermannweg 10, 55128 Mainz, Germany.

<sup>c</sup> Suzhou Niumag Analytical Instrument Corporation, Suzhou 215011, China.

<sup>d</sup> College of Materials Science and Engineering, Shenzhen Key Laboratory of Polymer Science and Technology, Guangdong Research Center for Interfacial Engineering of Functional Materials, Nanshan District Key Lab for Biopolymers and Safety Evaluation, Shenzhen University, Shenzhen 518055, China

<sup>e</sup> Shanghai Institute of Organic Chemistry, Chinese Academy of Sciences, Shanghai 200032, China

\*Corresponding Author: (Y. Yao) [yanzhch@szu.edu.cn](mailto:yanzhch@szu.edu.cn), [junfangli@sioc.ac.cn](mailto:junfangli@sioc.ac.cn), [yfyao@phy.ecnu.edu.cn](mailto:yfyao@phy.ecnu.edu.cn)

#### Contents:

- **<sup>1</sup>H spectra of PEO480 and PEO255 at different temperatures (Fig. S1)**
- **<sup>1</sup>H DQ data processing (Fig. S2)**
- **Obtaining polymer backbone order parameter distributions (Fig. S3)**
- **<sup>1</sup>H T<sub>2</sub> measurement and DQ NMR of PEO mixtures (Fig. S4)**
- **Rheology measurements of PEO255 at different temperatures (Fig. S5)**

## $^1\text{H}$ spectra of PEO480 and PEO255 at different temperatures

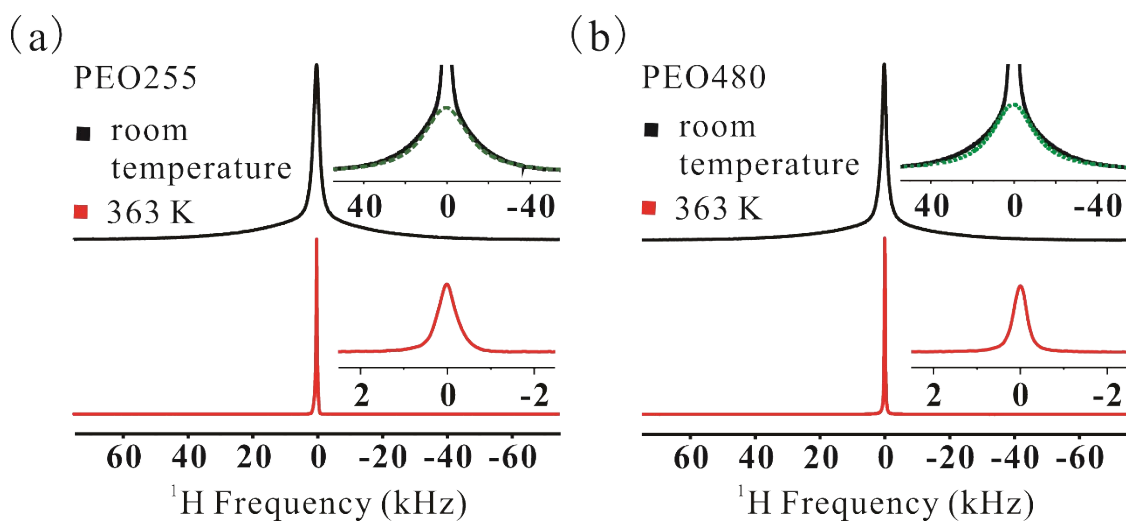


Fig. S1  $^1\text{H}$  NMR line shapes of samples PEO480 (a) and PEO255 (b) at room temperature and 363 K.

The  $^1\text{H}$  spectra of PEO255 and PEO480 polymers obtained at room temperature and at 363 K are presented in Figs. S1a and S1b, respectively. The results indicate that the spectra obtained for both polymers at room temperature consist of two components, including broad components, which are respectively fitted by dashed and dotted lines in Figs. S1a and S1b, and have full width at half maximum (FWHM) values greater than 20 kHz, while the narrow components have FWHM values lower than 3 kHz. The narrow and broad peaks can be attributed to non-crystalline and crystalline regions of the polymers, respectively. As expected, the peaks associated with the crystalline regions of the polymers disappear at 363 K, and the remaining signals are sharp peaks with FWHM values lower than 1 kHz, which are much narrower than those obtained at room temperature. These results verify that the PEO255 and PEO480 polymers are in a melt state at 363 K.

## <sup>1</sup>H DQ data processing

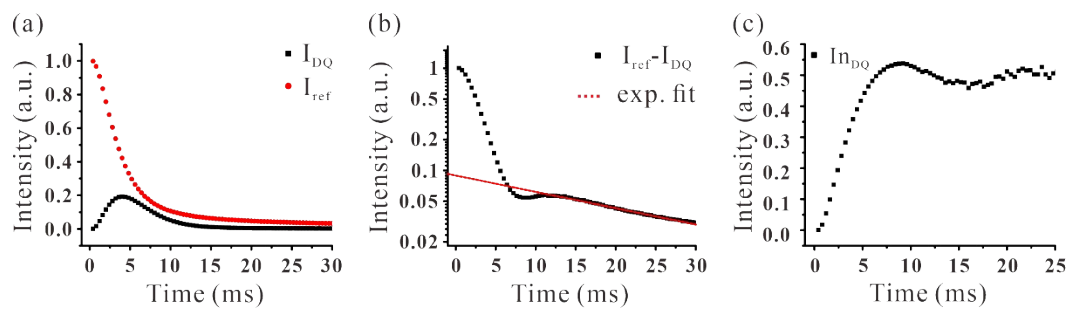


Fig. S2 (a) Experimental  $I_{DQ}$  and  $I_{ref}$  data measured as a function of double-quantum evolution time,  $\tau_{DQ}$ , for PEO480 at a fixed  $t_c$  value of 0.4 ms and a temperature of 363 K. (b) The difference of reference and DQ intensities ( $I_{ref} - I_{DQ}$ ) can be used to identify the more slowly relaxing nonelastic (isotropically mobile) fraction of the polymer structure by fitting the exponential relaxing tail. (c) The fraction of defects has to be subtracted to obtain the normalized DQ intensity  $In_{DQ}$  by taking the equation of  $In_{DQ} = I_{DQ} / (I_{DQ} + I_{ref} - defects)$ .

### Obtaining polymer backbone order parameter distributions

The distribution function  $f$  is solved via Tikhonov regularization<sup>1-3</sup> in the following form:

$$f = \operatorname{argmin}_{f \geq 0} \|Kf - I_{nDQ}\|^2 + \alpha \|f\|^2$$

Where  $\mathbf{f} = [f(1), f(2), \dots, f(N)]^T$  is the column vector of discrete distribution function,  $\mathbf{I}_{nDQ} = [I_{nDQ}(1), I_{nDQ}(2), \dots, I_{nDQ}(M)]^T$  is the column vector of normalized DQ build-up,  $\alpha$  is the error parameter, and  $\mathbf{K}$  is the inversion kernel matrix. For DQ data inversion, the element  $K_{mn}$  on the  $m$ -th row and the  $n$ -th column is:

$$K_{mn} = \frac{1}{2} \left( 1 - \exp\left[-\frac{2}{5} D_{res}(n)^2 \tau_{DQ}(m)^2\right] \right)$$

Where subscripts  $m$  ( $m = 1, 2, \dots, M$ ) and  $n$  ( $n = 1, 2, \dots, N$ ) are the indices of data points and discrete  $D_{res}$  values, respectively.

We have chosen the L-curve<sup>4</sup> method for optimal choice of error parameters since the method is well-established and has been widely used in regularization. A set of error parameters are tested and corresponding solutions ( $\mathbf{f}$ ) and fitting residuals ( $\boldsymbol{\chi} = [\chi(1), \chi(2), \dots, \chi(M)]^T = \mathbf{K}\mathbf{f} - \mathbf{I}_{nDQ}$ ) are recorded. The residual norm  $\chi^2$  ( $\chi^2 = \sum \chi(m)^2$ ) and solution norm  $f^2$  ( $f^2 = \sum f(n)^2$ ) are plotted in a log-log frame, forming a curve in the shape of the letter L. A critical point can be found from the L-curve and corresponding error parameter shall be picked for optimal solution. The procedures mentioned above applied to all DQ experiments (including PEO255 at the temperature of 393 K).

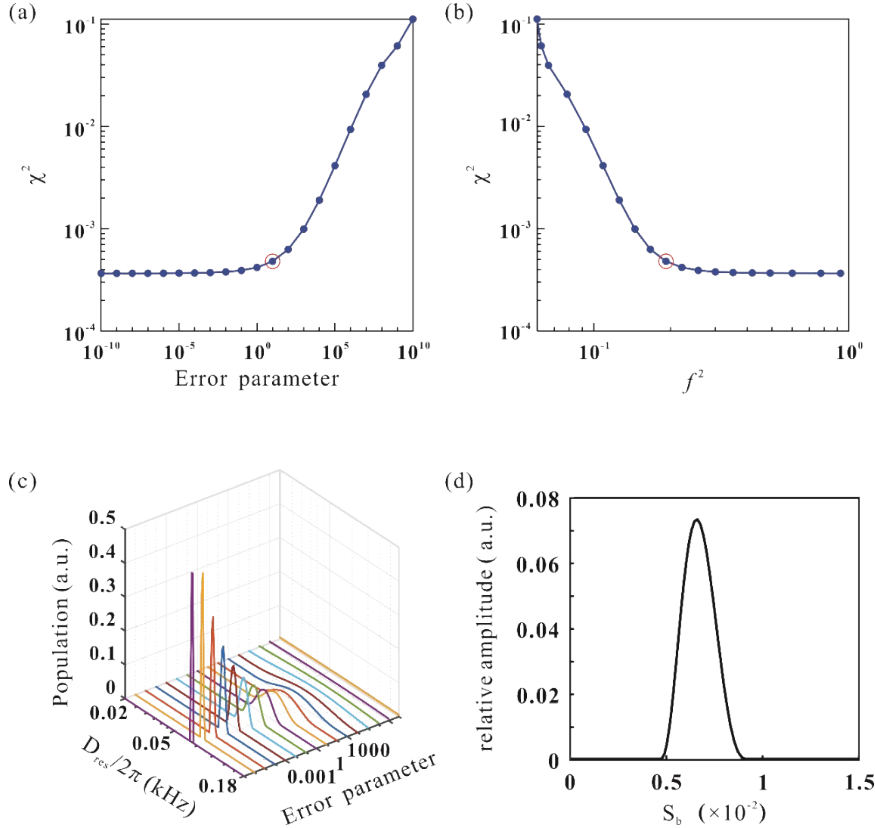


Fig. S3 Residual dipole coupling ( $D_{res}$ ) and backbone order parameter ( $S_b$ ) distributions obtained by Tikhonov regularization on normalized DQ data ( $I_{nDQ}$ ). (a)  $\chi^2$  (residual norm) as a function of multiple trial error parameters. Regularization techniques solve

such kind of ill-posed problems by finding a tradeoff between goodness of fit and reliability of solutions. Small error parameters achieve better fits but are at risk of yield unrealistic distributions with artifacts that should be avoided. An error parameter with corresponding  $\chi^2$  which is not too far, yet not too close to the best of fit [e.g. the point highlighted in a red circle in (a)] is usually considered to be reliable. (b)  $\chi^2$ (residual norm) as a function of  $f^2$  (solution norm) for optimal choice of error parameters, known as the L-curve method. The critical point of the L-curve was highlighted by a red circle. It represented the point highlighted in panel (a) as they have the same  $\chi^2$ . (c) Candidate  $D_{res}$  distribution solutions yielded by trial error parameters for PEO480 at the temperature of 363K. Unrealistically narrow peaks emerged as excessively small error parameters were being tested. The optimal solution yielded by the suggested error parameter ( $10^1$  in this case) shall be finally adopted. (d) The  $S_b$  distribution obtained from the optimal  $D_{res}$  distribution in (c).

### $^1\text{H}$ $T_2$ measurement and DQ NMR of PEO mixtures

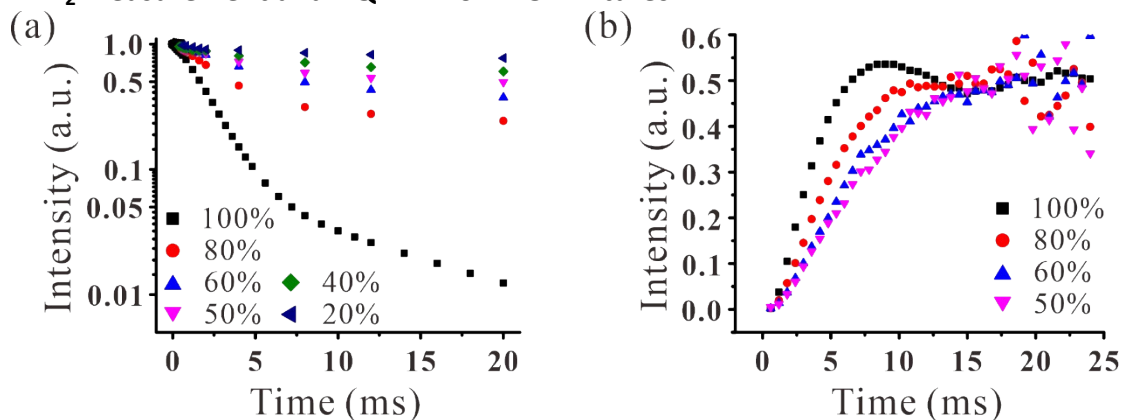


Fig. S4  $^1\text{H}$  NMR spectroscopy results for mixed PEO melts composed of PEO480 and PEO2 with different percentages of PEO480 by weight at a temperature of 363 K: (a)  $^1\text{H}$  NMR  $T_2$  relaxation decay curves; (b) DQ build-up curves. The results in (a) become increasingly nonlinear with an increasing proportion of PEO480, while the slope of the initially increasing segment in (b) increases as well.

## Rheology measurements of PEO255 at different temperatures

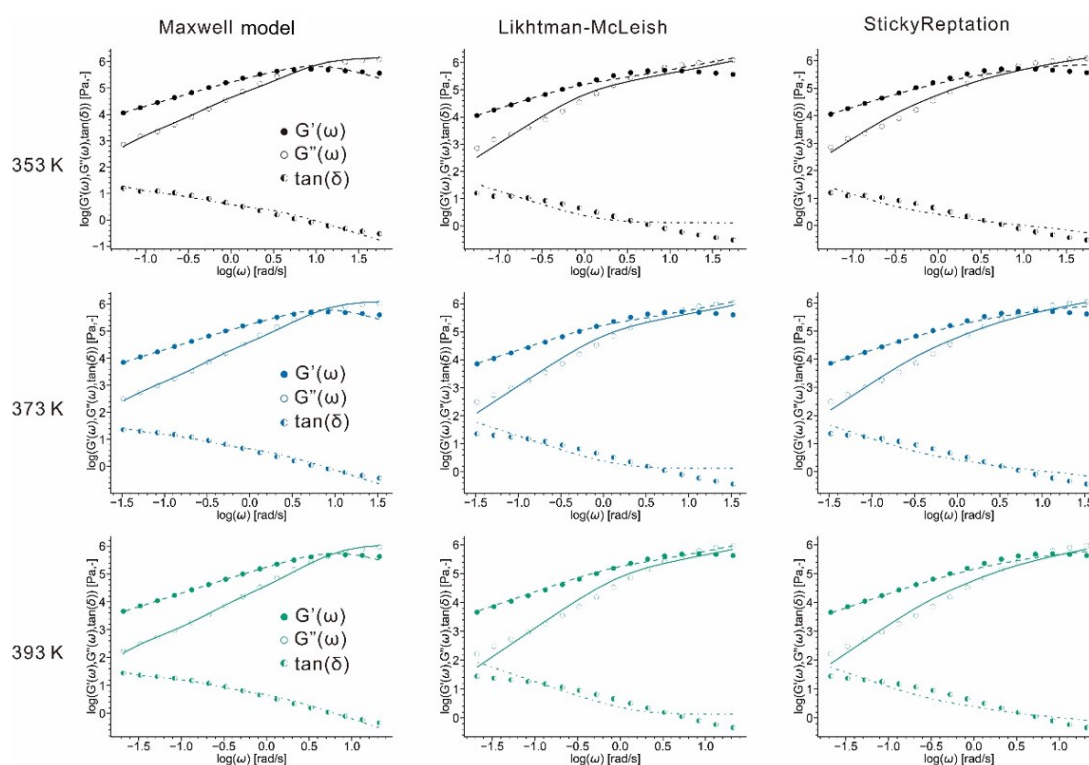


Fig. S5 Rheology data of PEO255 measured at 353, 373 and 393 K. The data were fitting using *RepTate rheology software* with the models of Maxwell (the number of element equal to 3), Likhtman–McLeish and StickyReptation, respectively.

## Notes and references

- [1] Tikhonov AN. Regularization of ill-posed problems. Dokl Akad Nauk SSSR **1963**,151, 49–52.
- [2] Tikhonov AN. Solution of incorrectly formulated problems and the regularization method. Dokl Akad Nauk SSSR **1963**, 151, 501–504.
- [3] Tikhonov AN, Arsenin VY. Solutions of ill-posed problems; John F, trans, New York, 1977.
- [4] Hansen PC. Rank-Deficient and Discrete ill-Posed Problems: Numerical Aspects of Linear Inversion; SIAM: Philadelphia, 1998.